JOC Article

Synthesis of Heterocyclic Analogues of Epibatidine via 7-Azabicyclo[2.2.1]hept-2-yl Radical Intermediates. 1. Intermolecular Reactions

Elena Gómez-Sánchez, Elena Soriano,† and José Marco-Contelles*

Laboratorio de Radicales Libres, IQOG (CSIC), C/Juan de la Cierva 3, 28006-Madrid, Spain

iqoc21@iqog.csic.es

Received May 23, 2008

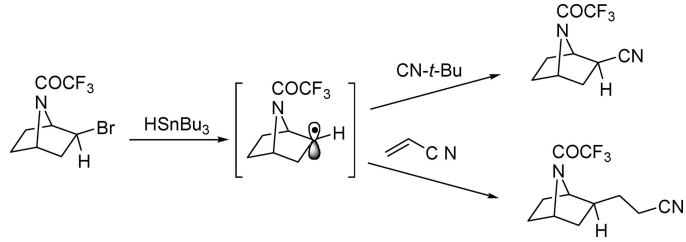

The synthesis and reactivity of the 7-azabicyclo[2.2.1]hept-2-yl radical has been extensively investigated in inter- and intramolecular reaction processes for the first time. In this work we will present the preparation of the radical and its successful intermolecular reaction with radical acceptors such as *tert*-butylisocyanide and acrylonitrile. Computational analyses have been carried out to show and explain the mechanisms and stereochemical outcome of these transformations. Overall and from the chemical point of view, a new and convenient synthetic approach has been developed for the synthesis of *exo*-2-(cyano)alkyl substituted 7-azabicyclo[2.2.1]heptane derivatives, a series of compounds of wide interest for the synthesis of heterocyclic analogues of epibatidine. As a result, we describe here the synthesis of the tetrazoloepibatidines (**8** and **15**) and the oxadiazoloepibatidine (**10**).

Introduction

The 7-azabicyclo[2.2.1]heptane is a common structural motif in a number of natural or non-natural products with interesting biological and pharmacological properties. This is the case of epibatidine[1] (Figure 1), an alkaloid isolated from the skin of the Ecuadorian poison frog *Epipedobates tricolor*,[2] which shows high affinity for the neuronal nicotinic acetylcholine receptor.[3] Consequently, a series of methodologies has been reported for the preparation of 7-azabicyclo[2.2.1]heptane derivatives.[4]

In a recent report from this laboratory, we described a simple and convenient method for the preparation of diversely 7-substituted *exo*-2-bromo-7-azabicyclo[2.2.1]heptane derivatives (**I**) based on a simple synthetic sequence starting from readily available cyclohex-3-enecarboxylic acid, Curtius reaction, stereoselective bromination leading to major 7-*tert*-butyl (benzyl) 7-(*c*-3,*t*-4-dibromocyclohex-1-yl)carbamates (or 2,2,2-trifluoroacetamides), followed by DMF/sodium hydride-mediated intramolecular cyclization (Scheme 1).[5]

The ready access to compounds of type **I** moved us to use these derivatives as suitable precursors for the synthesis of new heterocyclic analogues of epibatidine[6] for biological evaluation. We were particulaly interested in the new heterocyclic analogues of epibatidine such as triazolo- (**II**) and tetrazoloepibatidine (**III**) (Figure 1), whose chemistry and pharmacology has been scarcely developed and investigated.[7]

† To whom correspondence should be addressed about computational chemistry. E-mail: esoriano@arrakis.es.

(1) For some selected reviews on the chemistry and biology of epibatidine and analogues, see: (a) Daly, J. W. *J. Med. Chem.* **2003**, *46*, 445. (b) Romanelli, M. N.; Gualteri, F. *Med. Res. Rev.* **2003**, *23*, 393. (c) Broka, C. A. *Med. Chem. Res.* **1994**, *4*, 449.

(2) Spande, T. F.; Garraffo, H. M.; Edwards, M. W.; Yeh, H. J. C.; Pannell, L.; Daly, J. W. *J. Am. Chem. Soc.* **1992**, *114*, 3475.

(3) Holladay, M. W.; Dart, M. J.; Lynch, J. K. *J. Med. Chem.* **1997**, *40*, 4169.

(4) Chen, Z.; Trudell, M. L. *Chem. Rev.* **1996**, *96*, 1179.

(5) (a) Gómez-Sánchez, E.; Soriano, E.; Marco-Contelles, J. *J. Org. Chem.* **2007**, *72*, 8656 See also: (b) Bastable, J. W.; Cooper, A. J.; Dunkin, I. R.; Hobson, J. D.; Riddell, W. D. *J. Chem. Soc, Perkin Trans 1* **1981**, 1339. (c) Kapferer, P.; Vasella, A. *Helv. Chim. Acta* **2004**, *87*, 2764. (d) Casabona, D.; Jiménez, A. I.; Cativiela, C. *Tetrahedron* **2007**, *63*, 5056.

(6) (a) Carroll, F. I. *Bioorg. Med. Chem. Lett.* **2004**, *14*, 1889. (b) Seerden, J.-P. G.; Tulp, M. Th. M.; Scheeren, H. W.; Kruse, C. G. *Bioorg. Med. Chem.* **1998**, *6*, 2103.

(7) (a) Shen, T. Y.; Harman, W. D.; Huang, D. F.; González, J. US(1998)5817679. (b) Shen, T. Y.; Harman, W. D.; Huang, D. F.; González, J. WO(1996 9606093.

10.1021/jo8011094 CCC: $40.75
Published on Web 07/26/2008

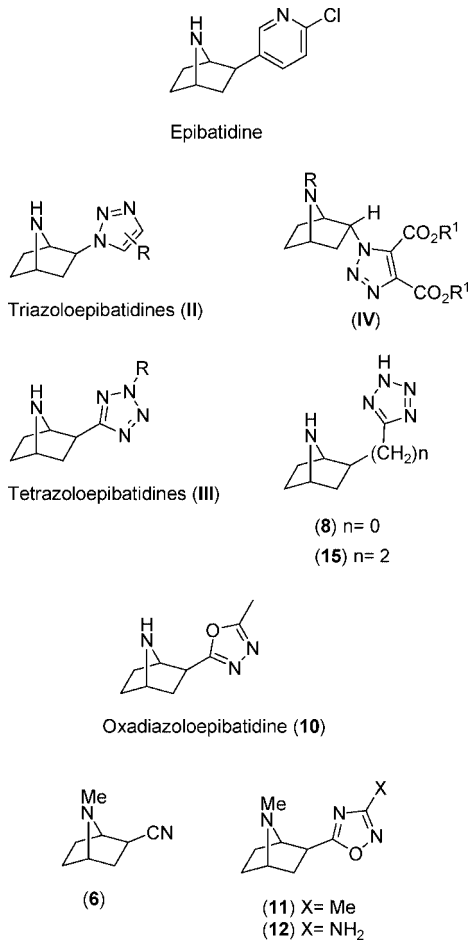

FIGURE 1

SCHEME 1

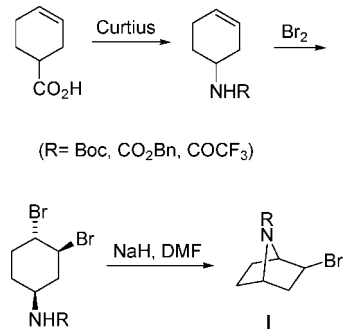

Targeting our initial efforts to the triazoloepibatidines (**II**) (Figure 1) and considering our precursors (**I**) (Scheme 1), a simple synthetic approach was devised based on simple sodium azide nucleophilic displacement of the bromine atom at C2, followed by 1,3-dipolar cycloaddition reaction with an appropriate alkyne. This route gave the azide intermediate and the expected heterocycles (**IV**: R = BOC, H, R^1 = Me) (Figure 1) in low overall yield and with the *endo* configuration at C2, the wrong orientation for biological purposes (see Supporting Information).[8a] The attempted epimerization of substrate **IV** (R = BOC, R^1 = Me) at C2, under conditions[8b] that proved useful in the epimerization of *endo*- to *exo*-epibatidine, did not afford the expected product.[8c] Thus, an alternative synthetic pathway was sought.

We soon realized that free radical chemistry on radical species derived from compounds **I** (Scheme 1) could be an interesting option in order to achieve the synthesis of useful intermediates for our target molecules. We were particularly surprised to see that although the synthesis and reactivity of 7-norbornenyl,[9] norborn-5-en-2-yl,[10] and norborn-2-yl[11] radicals are well-known, the chemistry of the 7-azabicyclo[2.2.1]hept-2-yl radical has been scarcely investigated.[12,13] In the 1970s Fraser and Swingle reported the chlorination of 7-trichloroacetyl-7-azabicyclo[2.2.1]heptane with sulfuryl chloride in the presence of benzoyl peroxide to give the *exo*-2-chloro derivative in 31% yield,[12a] while more recently Armstrong and co-workers have reported the low yielding $Ni(COD)_2$-mediated intramolecular cyclization of *exo*-2-bromo-7-(toluene-4-sulfonyl)-7-azabicyclo[2.2.1]heptane, as well as the intermolecular free radical bromodecarboxylation of Barton thiohydroxamic esters.[13] These facts prompted us to embark in a project to investigate the inter- and intramolecular free radical reactions of precursors **I** (Scheme 1).

Consequently, continuing with our interest on the synthesis of triazoloepibatidines (**II**, Figure 1) (see above), the free radical azidation[14] reaction of precursor **1** (R = $COCF_3$) (Scheme 1) was the obvious issue for the synthesis of the key azide intermediate, but in the usual conditions and using ethanesulfonylazide in the presence of dilauryl peroxide[14a] or other similar conditions,[14b] we were unable to obtain the desired 2-azido derivative; as a result, we stopped here our synthetic approches to triazoloepibatidines and directed our efforts to the synthesis of the analogous tetrazoloepibatidines.

In this manuscript we will show the successful results that we have obtained in the intermolecular reactions of precursors **I** with *tert*-butylisocyanide and acrylonitrile, to give the key intermediates (**2**, **13**) for the synthesis of tetrazoloepibatidines **8/15** and oxadiazoloepibatidine **10** (Figure 1). When necessary and possible we have extensively used computational chemistry (DFT analysis) to explain the observed steroselectivities or to rationalize the proposed reaction mechanisms.

Analogously, the intramolecular reactions of suitable substituted precursors **I** (Scheme 1) will be described elsewhere.[15]

(8) (a) Gómez-Sánchez, E.; Marco-Contelles, J. *Lett. Org. Chem.* **2006**, *3*, 827. (b) Leen, C.-L. K.; Loh, T.-P. *Org. Lett.* **2005**, *7*, 2965. (c) Gassman, P. G.; Schenk, W. N. *J. Org. Chem.* **1977**, *42*, 918.

(9) Underwood, G. R.; Friedman, H. S. *J. Am. Chem. Soc.* **1977**, *99*, 27.

(10) (a) Giese, B.; Jay, K. *Chem. Ber.* **1979**, *112*, 298. (b) Srikrishna, A.; Viswajanani, R.; Reddy, T. J.; Vijaykumar, D.; Kumar, P. P. *J. Org. Chem.* **1997**, *62*, 5232. (c) Liaw, D.-J.; Huang, C.-C.; Ju, J.-Y. *J. Polym. Sci., Part A* **2006**, *44*, 3382.

(11) Boivin, J.; da Silva, E.; Ourisson, G.; Zard, S. *Tetrahedron Lett.* **1990**, *31*, 2501. (b) Takasu, K.; Mizutani, S.; Nogushi, M.; Makita, K.; Ihara, M. *Org. Lett.* **1999**, *1*, 391.

(12) (a) Fraser, R. R.; Swingle, R. B. *Can. J. Chem.* **1970**, *48*, 2065. (b) Given the suitable spatial arrangement of the CF_3 moiety towards a possible intramolecular migration of a fluorine atom to the radical center, we have carried out the theoretical study of this step in order to evaluate its competitiveness in the reaction conditions. As shown by the calculations, this is an endothermic process ($\Delta G = 5.0$ kcal mol^{-1}) with a very high free activation energy, $\Delta G^{\ddagger}$, of 55.0 kcal mol^{-1} (activation enthalpy, $\Delta H^{\ddagger} = 53.1$ kcal mol^{-1}). A comparison with the calculated values for the intermolecular reaction ($\Delta G^{\ddagger} \approx 20$ kcal mol^{-1}) shows that this process appears to be clearly unfavored and hardly achievable in the reaction conditions.

(13) Armstrong, A.; Bhonoah, Y.; Shanahan, S. E. *J. Org. Chem.* **2007**, *72*, 8019.

(14) (a) Ollivier, C.; Renaud, P. *J. Am. Chem. Soc.* **2000**, *122*, 6496. (b) The tested conditions included (i) ethanosulfonylazide, AIBN and slow addition of $HSnBu_3$ in toluene under reflux, (ii) ethanosulfonylazide, AIBN, $ClSnBu_3$, $NaBH_3CN$ in *t*BuOH at 100 °C, and (iii) sodium azide, AIBN and $ClSnBu_3$ in toluene under reflux. In all cases the starting material was either recovered unchanged or detected by ^{1}H NMR as the major product.

(15) Reference deleted in proof.

SCHEME 2

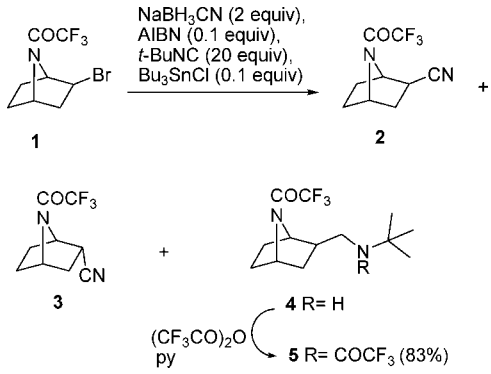

Results and Discussion

Reaction of Compound 1 with *tert*-Butylisonitrile. For the synthesis of the tetrazoloepibatidines (**III**, Figure 1),[16] we investigated the reaction of trimethylsilylazide or any other azide surrogate[17] with the appropriate *exo*-2-cyano derivative (**2**, Scheme 2). In order to obtain this compound, the intramolecular reaction of compound **1** with *tert*-butylisocyanide, a classic for the synthesis of nitriles from alkyl halides,[18] was analyzed.[19] After extensive investigation (see Supporting Information), experimental conditions were found for a convenient and reproducible reaction giving major *exo*-2-cyano derivative **2** in 38% yield (Scheme 2) (see Experimental Section). Unfortunately, this moderate yield is in agreement with the low yield recorded for the intermolecular free radical chlorination of a related precursor.[12a] An intramolecular fluorine migration has also been excluded to explain the low yields of compound **2**.[12b] Compound **2** was obtained accompanied with traces of minor *endo*-2-cyano isomer **3** and amine **4** (Scheme 2). The structure of *tert*-butylamine **4** has been confirmed by its analytical and spectroscopic data, as well as by reaction with trifluoroacetic anhydride to give the bis-trifluoroacetamide **5** (Scheme 2). The relative configuration at the new formed stereocenters has been easily established by ^{1}H NMR analysis measuring the vicinal coupling constants between H(C1)−H(C2) and H(C2)−H(C3) and by comparison with the data reported in the literature for related *exo*-2-cyano-7-methyl-7-azabicyclo[2.2.1]heptane (**6**) (Figure 1), obtained by osmium-promoted 1,3-dipolar cycloaddition between acrylonitrile and *N*-substituted pyrroles.[20]

The formation of major *exo*-C2 isomer **2** was expected,[12a] but the isolation of *exo*-C2 amine **4** has no precedent, and to the best of our knowledge this is the first time that such a product has been described in the intermolecular reaction of carbon radicals with *tert*-butylisocyanide. Accordingly, we have carried out a computational analysis aimed at (a) explaining the high stereoselection of this reaction favoring *exo*-isomers and (b) giving support to the mechanistic hypothesis shown in Scheme 3 to rationalize the formation of compound **4**, besides **2** and **3**.

SCHEME 3

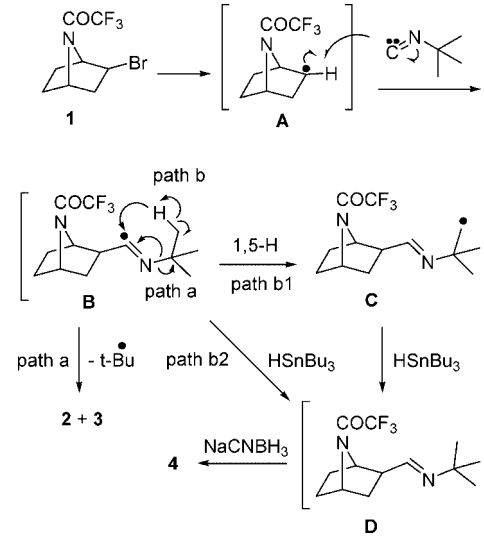

SCHEME 4

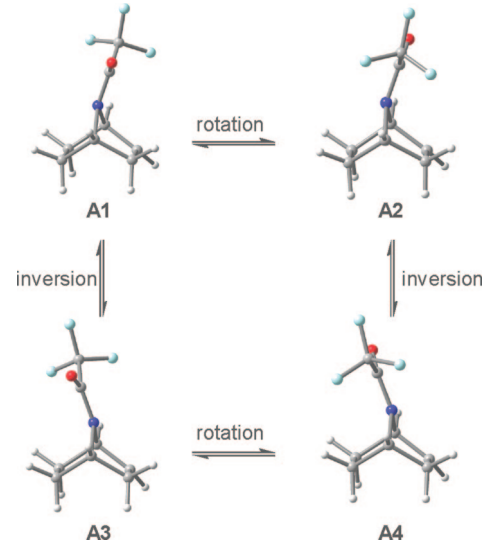

Mechanism of the Reaction of Compound 1 with *tert*-butylisocyanide. It is well-known that the amide group of bicyclic 7-azabicyclo[2.2.1]heptane is nitrogen pyramidal.[21] Therefore, two kind of geometrical transformations with respect to the amide bond can occur, giving rise to up to four radical conformers: (1) bond rotation around the C(O)-N linkage; and (2) nitrogen inversion (Scheme 4). It could be argued that a high pyramidalization could inhibit the *exo*-attack on conformer **A1** and, to a lesser extent, on **A2** as a result of the increased steric hindrance to the incoming group.

To get insight into the influence of the amide conformation on the reactivity and selectivity of the radical, we have studied both conformational transformations.[22] The calculated rotational

(16) Herr, R. J. *Bioorg. Med. Chem.* **2002**, *10*, 3379.

(17) (a) Duncia, J. V.; Pierce, M. E.; Santela, J. B., III *J. Org. Chem.* **1991**, *56*, 2395. (b) Wittenberger, S. J.; Donner, B. G. *J. Org. Chem.* **1993**, *58*, 4139. (c) Himo, F.; Demko, Z. P.; Noodleman, L.; Sharpless, K. B. *J. Am. Chem.* **2003**, *125*, 9983. (d) Amantini, D.; Beleggia, R.; Fringuelli, F.; Pizzo, F.; Vaccaro, L. *J. Org. Chem.* **2004**, *69*, 2896. (e) Rauter, A. P.; Padilha, M. *J. Carbohydr. Chem.* **2005**, *24*, 275. [when using this method, NH_4Cl/NaN_3, the reaction was incomplete and the yield of compound **7** was 12% (28%)].

(18) (a) Stork, G.; Sher, P. M. *J. Am. Chem.* **1986**, *108*, 303. (b) Blum, D. M.; Roberts, B. P. *J. Chem. Soc., Perkin Trans. 2* **1978**, 1313.

(19) Product **2** could not be obtained by S_N2 reaction of compound **1** with excess sodium cyanide in DMF at reflux. This is further supported by theoretical calculations, which have shown a very high $\Delta G^{\ddagger}$ for the process (40.10 kcal mol^{-1}), probably due to a defficient orbital overlap arising from steric strain. An NBO analysis has revealed that the steric hindrance for the incoming CN^- gives rise to a defficient overlap between the lone pair orbital and the σ^*_{C-Br} that reduces the interaction energy in the transition state.

(20) González, J.; Koontz, J. I.; Hodges, L. M.; Nilsson, K. R.; Neely, L. K.; Myers, W. H.; Sabat, M.; Harman, W. D. *J. Am. Chem. Soc.* **1995**, *117*, 3405.

(21) Ohwada, T.; Achiwa, T.; Okamoto, I.; Shudo, K. *Tetrahedron Lett.* **1998**, *39*, 865.

(22) See Supporting Information for etails.

barriers were found to be moderately low (15 kcal mol^{-1}) as compared with those of acyclic amides (21.37 kcal mol^{-1}), while the inversion barriers were considerably smaller (~1 kcal mol^{-1}), thus suggesting that rotation is a rate-limiting process in the conformational space. The decrease in the rotational barriers for bicyclic versus acyclic amides is due to a loss of the resonance stabilization, i.e., the delocalization stabilization of the lone pair electrons of N from the nonbonding n_N orbital to the antibonding $\pi^*_{C=O}$ orbital.[23] The strained bicyclo[2.2.1]heptane skeleton induces a distortion on the N environment and hence on the nonbonding orbital, which may inhibit the efficient delocalization of the lone pair.

On the basis of these results, it could be argued that the approach of *tert*-butylisonitrile to conformers **A1** and **A2** would not be so impeded by steric hindrance as one might suppose because a very fast *N*-inversion could take place to allow the reaction.

On other hand, in most of the carbon-centered free radicals the unpaired electron occupies an orbital that has mainly p-character (i.e., they are π radicals), allowing attack from two sides. However, torsional and stereoelectronic effects influence the diastereoselectivity of reactions of cyclic radicals such as **A** (Scheme 3). It has been long demonstrated by theoretical studies[24] that radicals are pyramidalized when substituted by alkyl groups in conformations that are asymmetric with respect to the plane of the trigonal center and the three attached substituents and that this pyramidalization is strongly dependent on conformational effects. Thus, when the bond angle formed by the substituents is strained to a value smaller than 120°, such as in small or highly constrained rings like norbornyl-type adducts, the pyramidalization is manifest. In radical species **A**, the substitution of the bridging methylene group with a heteroatom in the aza-derivative increases the effective electronegativity of C_1 and also implies shorter bonds with C_1 and C_4 than in a carbocycle, which induces a further closing of the $C_1-C_2-C_3$ bond angle and hence a distortion to a more pyramidal geometry around the radical center.[25]

The DFT optimized geometry of conformers **A1**−**A4** assigns a slight pyramidal character for the radical-center carbon with the C_2-H bond bent in the *endo* direction, so the two faces should no longer be equivalent and the radical intermediates would preferentially undergo an *exo*-attack, as was found experimentally for the 2-norbornyl radical.[25] The calculated geometric parameters (see Table 5 in Supporting Information) evidence the radical-center pyramidalization, always to the *endo*-direction, in agreement with the staggering effect proposed by Houk.[26,27] According to this postulate, a planar tricoordinate atom placed in an unsymmetrical environment will pyramidalize toward a staggered conformation.

In line with this, the NBO analysis indicates[22] that the staggering effect results in tilting of the singly occupied orbital and pyramidalization, which improves overlap and favors hyperconjugative interactions with the bonds which lie in the same plane. Therefore, torsional effects and hyperconjugation are both reinforcing,[28] promoting pyramidalization to the *endo* direction.

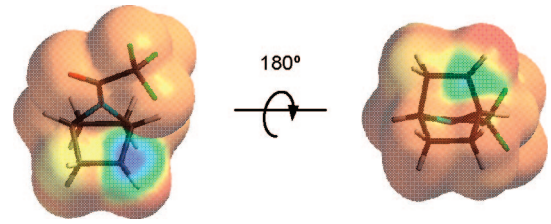

FIGURE 2. Spin density computed on the van der Waals surface for **A1**, seen from two perspectives (*exo*-face, left; *endo*-face, right). Regions with the largest spin density are colored in blue.

The calculation of other electronic parameters reveals that the SOMO (single-occupied molecular orbital) on **A1**−**A4** appears mainly located over C_2, whereas the SOMO map computed on the van der Waals surface shows a preferential concentration on the *exo*-face (Chart 2 in Supporting Information). This is consistent with the spin density maps (Figure 2) which clearly show that *exo*- and *endo*-faces are nonequivalent, the spin density being larger in the *exo*-face.

To get further insights into the stereoselectivity of the 7-aza-norborn-2-yl radical **A**, we optimized the eight plausible transition structures for the addition of *tert*-butylisonitrile to the four conformers **A1**−**A4** over the *exo*- and *endo*-faces. The results indicate that the amide group exerts important structural effects on the course of the reaction over the *exo*-face. Thus, conformers **A1** and **A3**, interchangeable by N inversion, yield the same adduct ($\mathbf{B1_x} = \mathbf{B3_x}$, see Chart 3 in Supporting Information). The transition structure for **A3** ($\mathbf{TS_{A3x}}$) shows N inversion, hence being the same as for **A1** ($\mathbf{TS_{A1x}}$). The inversion found in $\mathbf{TS_{A3x}}$ is due to the formation of a weak H-bond between the carbonyl oxygen and a proton at *tert*-butyl moiety, which probably induces an even faster inversion and lightly stabilizes the transition structure. Once the transition structure is reached, it undergoes a spontaneous N inversion upon optimization to the subsequent intermediate to alleviate the steric interactions with the *tert*-butylisonitrile. The same relationship is also observed between conformers **A2** and **A4**, and unfavorable steric effects may be overcome by a kinetically easy N inversion on the aza-norbornyl framework.

The *endo*-counterparts lack interactions involving the amide carbonyl, so the initial N pyramidalization is kept along the reaction coordinate (see Figure 4 for the process over both faces for **A2**).

The computed results, summarized in Table 1, indicate that the reaction over the *exo*-face requires enthalpies of activation 1.5−2 kcal mol^{-1} lower than over the *endo*-face both in the gas phase and in solution. Additionally, whereas the former is a slightly exothermic process, the *endo*-attack is endothermic by ~4 kcal mol^{-1} for all the conformers.

(23) Otani, Y.; Nagae, O.; Naruse, Y.; Inagaki, S.; Ohno, M.; Yamaguchi, K.; Yamamoto, G.; Uchiyama, M.; Ohwada, T. *J. Am. Chem. Soc.* **2003**, *125*, 15191.

(24) (a) Pacansky, J.; Dupuis, M. *J. Chem. Phys.* **1978**, *68*, 4276. (b) Pacansky, J.; Dupuis, M. *J. Chem. Phys.* **1979**, *71*, 2095. (c) Pacansky, J.; Dupuis, M. *J. Chem. Phys.* **1980**, *73*, 1867. (d) Yoshimine, M.; Pacansky, J. *J. Chem. Phys.* **1981**, *74*, 5168. (e) Paddon-Row, M. N.; Houk, K. N. *J. Am. Chem. Soc.* **1981**, *103*, 5046.

(25) Kawamura, T.; Koyama, T.; Yonezawa, T. *J. Am. Chem. Soc.* **1973**, *95*, 3220.

(26) (a) Rondan, N. G.; Paddon-Row, M. N.; Caramella, P.; Mareda, J.; Mueller, P. H.; Houk, K. N. *J. Am. Chem. Soc.* **1982**, *104*, 4974. (b) Houk, K. N.; Rondan, N. G.; Brown, F. K.; Jorgensen, W. L.; Madura, J. D.; Spellmeyer, D. C. *J. Am. Chem. Soc.* **1983**, *105*, 5980.

(27) A pioneering work by Schleyer focused attention on the relief of torsional strain involving the bridgehead CH bond in norbornyl systems and noted the general role of the transition-state torsional interactions: Schleyer, P. v. R. *J. Am. Chem. Soc.* **1967**, *89*, 701. For other works on the "torsional effect", see: (a) Bartlett, P. D.; Fickes, G. N.; Haupt, F. C.; Helgeson, R. *Acc. Chem. Res.* **1970**, *3*, 177. (b) Huisgen, R.; Ooms, P. H. J.; Mingin, M.; Allinger, N. L. *J. Am. Chem. Soc.* **1980**, *102*, 3951. (c) Watson, W. H.; Galloy, J.; Bartlett, P. D.; Roof, A. A. M. *J. Am. Chem. Soc.* **1981**, *103*, 2022.

(28) Paddon-Row, M. N.; Houk, K. N. *J. Phys. Chem.* **1985**, *89*, 3771.

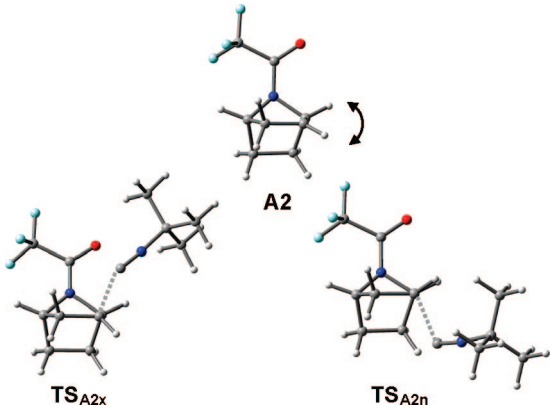

FIGURE 3. Staggering effect in the free-radical species **A2** (top) and in the transition structure for the *exo*- (bottom, left) and *endo*-attack (bottom, right).

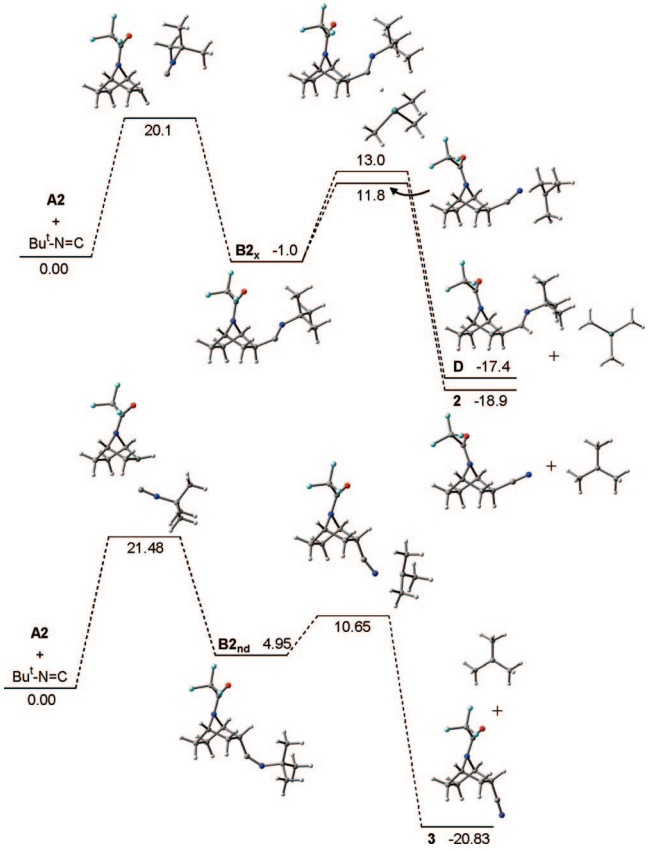

FIGURE 4. Free-energy profile in solution (kcal mol^{-1}) for the process over the *exo*- (top) and *endo*-face (bottom) for **A2**. For the *exo* process, the formation of **2** and the more favorable path to **D** (to amine **4**, path b2 of Scheme 3) are shown for comparison.

This step is accompanied by a minor charge transfer from the butylisonitrile to the aza-norbornyl species (0.06*e*),[22] so it is not a driving force, and the steric properties have a more pronounced effect for governing the selectivity, as predicted by Houk's model. The spin density computed reveals an evident decrease of the spin density on the bicycle in favor of the nitrile carbon and nitrogen atoms on going from the reactant species to the transition structure.[22] Remarkably, this effect is stronger for the *exo*-attack, thus supporting a more advanced reaction for the *exo*-attack in the transition state, consistent with the C−C forming bond length (2.198 Å for the transition structure of the *exo*- vs 2.204−2.209 Å for the *endo*-attack).

TABLE 1. Thermodynamic Data (kcal mol^{-1}) in Gas Phase and in Solution (*t*-BuOH) for Reaction on *exo*- and *endo*-Faces for Conformers A1−A4

conformer	addition face	$\Delta H^{\ddagger}_{gas}$	ΔH_{gas}	$\Delta G^{\ddagger}_{gas}$	ΔG_{gas}	$\Delta G^{\ddagger}_{sol}$	ΔG_{sol}
A1	*exo*	5.3	−19.0	16.1	−6.1	19.6	−0.9
	endo	7.3	−12.3	17.9	0.1	21.1	4.4
A2	*exo*	4.2	−18.9	16.5	−7.4	20.1	−1.0
	endo	7.5	−12.1	18.0	0.1	21.5	4.9
A3	*exo*	5.2	−19.1	16.0	−6.3	20.2	−0.3
	endo	7.6	−12.2	18.1	−0.2	21.8	3.8
A4	*exo*	4.1	−19.1	16.3	−7.5	19.7	−1.9
	endo	7.5	−12.0	18.1	−0.1	21.2	3.7

The bending of the C_2−H bond in the *endo* direction results in tilting of the odd electron orbital on C_2 in the *exo* direction, which is supported by the electronic analysis described above. If the C_2−H bond tilted toward the opposite *exo* direction, this bond would eclipse the C_1-H bond at or near the transition state during the radical transfer from the *endo* side (Figure 3). In contrast, the bending of the C_2−H bond in the *endo* direction releases the repulsive energy with the C_1−H bond, and the forming bond is situated nearly in the ideal staggered position in the transition state.

In summary, the pyramidalization of the free-radical species **A** and the fact that the *exo*-transition state is more stable can be both rationalized on the common basis of the preference of staggered conformations of vicinal bonds and the stabilizing effects of hyperconjugation.

The final fragmentation and formation of the 2-substituted aza-norbornyl derivative (**2** and **3**, path *a*, Scheme 3) and the pyramidalyzed *tert*-butyl radical[24e] is strongly exothermic, whatever face is attacked, and proceeds with a moderately low energy barrier (Figure 4). The transition state for the *endo* adduct appears slightly earlier than the *exo* adduct, as suggested by the breaking bond length (1.942 and 1.987 Å), probably promoted by the unfavorable steric interactions between the *tert*-butyl group and the protons at C_2 and C_3 in the less stable *endo* intermediate **B2$_{nd}$**. Two alternative pathways can be envisioned to justify the unexpected formation of amine **4** (Scheme 3): path *b1*, through an intramolecular homolytic 1,5-H shift from the intermediate **B**, followed by hydrogenation of **C** to generate the imine **D**; and *b2*, via direct hydrogenation of radical **B** to **D**. The direct tranformation to **D** is an exothermic step (by −16.4 kcal mol^{-1} from **B**), and the energy barrier to reach the transition structure (Sn−H = 1.874; C−H = 1.706 Å) is only 1.2 kcal mol^{-1} higher than that for the fragmentation step from **B**. In contrast, the intramolecular H-transfer has been found to be an endothermic step (8.0 kcal mol^{-1} from **B**) and takes place with a moderately high energy barrier (25.2 kcal mol^{-1} from **B**; 24.1 kcal mol^{-1} from the reactant structures). Clearly, these results suggest that the kinetic and thermodynamic preferred route to the formation of amine **4** proceeds through a direct reduction of **B** to **D** (path *b2*, Scheme 3). The high viscosity of *t*-BuOH may also partially account for the competitiveness of the formation of **4** versus the thermodynamically and slightly kinetically preferred fragmentation to yield nitrile **2**.

Synthesis of Tetrazoloepibatidine 8 and Oxadiazoloepibatidine 10. With compound **2** in hands, we next addressed the synthesis of tetrazole **8**. Several methods were assayed[17a–d] with variable results,[17e] the best one being that reported by Wittenberger and Donner[17b] using trimethylsilyl azide and dibutyltin oxide, which afforded compound **7** in 87% yield

SCHEME 5

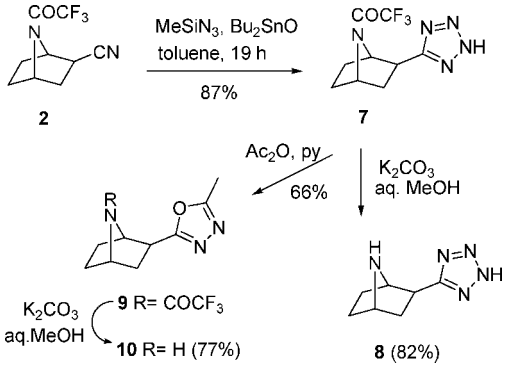

SCHEME 6

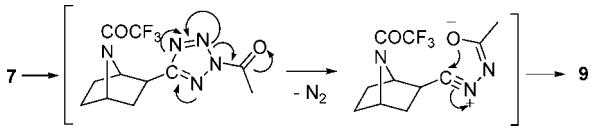

(Scheme 5). Basic hydrolysis under standard conditions removed the trifluoroacetyl group giving free tetrazole **8** in 82% yield (Scheme 5).

To prepare the *N*-acetyl derivative of tetrazole **7**, we treated this compound with acetic anhydride. However, instead of the *N*-acetyl derivative,[29] we isolated a new product whose analytical and spectroscopic data were in good agreement with the *exo*-C2 substituted 5-methyl-1,3,4-oxadiazole derivative **9** (Scheme 5). Similarly and as above, basic hydrolysis provided the free C2-substituted oxadiazole **10** in 77% yield (Scheme 4). In fact, this is the usual reactivity that one can expect during the acetylation of 2*H*-tetrazoles according to previous reports (Scheme 6).[30] It is interesting to note that related 1,2,4-oxadiazoles (**11**, **12**) (Figure 1) have been reported as muscarinic analgesics derived from epibatidine.[31]

Reaction of Compound 1 with Acrylonitrile. The moderate success observed in the intermolecular free radical reaction of precursor **1** with *tert*-butylisocyanide prompted us to analyze a similar reaction with a more powerful radical acceptor like acrylonitrile. In addition, a homologated nitrile such as **13** (Scheme 7) could be very useful in order to compare its biological profile with tetrazole **8** (Scheme 5) and accordingly establish a useful biological SAR.

Intermolecular free radical reaction of compound **1** with acrylonitrile, under the usual experimental conditions,[32] afforded the expected *exo*-C2 substituted diastereomer **13** in 38% yield. Fortunately, when changing the concentration of the reactive solution from 0.02 to 0.4 M, an excellent yield of the expected product **13** (87%) was obtained. Finally, a similar synthetic sequence as described for compound **10** (Scheme 5), gave tetrazole **15** via *N*-trifluoroacetamide **14** (Scheme 7) in good overall yield.[33]

SCHEME 7

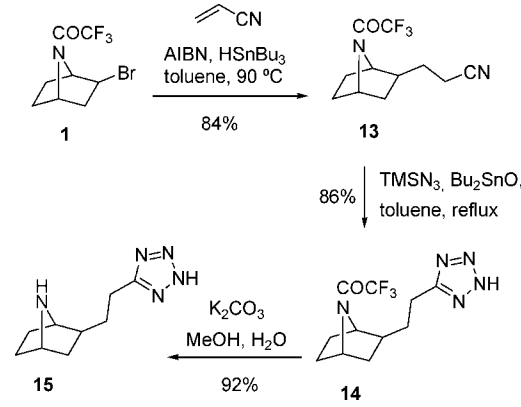

Conclusions

To sum up, in this work we have reported the synthesis and reactivity of the 7-azabicyclo[2.2.1]hept-2-yl radical, investigating its intermolecular reactions with radical acceptors such as *tert*-butylisocyanide and acrylonitrile. Based on the readily available radical precursor **1**, we observed that the efficiency of the radical reaction depends on the type of the radical acceptor, the best process being the Michael reaction with acrylonitrile, although we were unable to manage the free radical azidation or allylation reactions. The reaction with *tert*-butylisocyanide gave the expected *exo*-2-cyano derivative **2** (Scheme 1). In all of these transformations major or single *exo*- isomers were detected, conveniently isolated, and characterized. Overall and from the chemical point of view, a new and convenient synthetic approach has been developed for the synthesis of *exo*-2-(cyano)alkyl substituted 7-azabicyclo[2.2.1]heptane derivatives, a series of compounds of interest for the synthesis and biological evaluation of heterocyclic analogues of epibatidine. As a result, we have described here the synthesis of suitable intermediates (**2**, **7**, **13**, **14**, and **9**) for the preparation of new epibatidine heterocyclic analogues such as the tetrazoloepibatidines (**8**/**15**) and the oxadiazoloepibatidine (**10**).

A theoretical DFT-based study has been carried out to account for the stereochemical outcome of these reactions. The results show a slight pyramidalization (16−20°) of the odd electron orbital to the *endo* direction in the radical intermediate **A**, promoted by torsional and hyperconjugation effects. This pyramidalization induces a kinetically favored attack over the *exo*- rather than the *endo*-face, as the computed energy barriers reveal, giving rise to the high stereoselection found for these transformations.

Experimental Section

General Methods. Melting points were determined on a Kofler-type microscope and are uncorrected. ^{1}H NMR and ^{13}C NMR spectra were recorded at room temperature in $CDCl_3$, at 300, 400 or 500 MHz and at 75, 100 or 125 MHz, respectively, using solvent peaks ($CDCl_3$: 7.27 (*D*), 77.2 (*C*) ppm; D_2O 4.60 ppm) as internal reference. The assignment of chemical shifts is based on standard NMR experiments (^{1}H, ^{13}C, ^{1}H−^{1}H COSY, ^{1}H−^{13}C HSQC, HMBC). In the NMR spectra values with (*) can be interchanged. Duplicated signals indicate the presence of invertomers; values with (′) or (♦) show the invertomers, when distinguishable. GC-MS analyses were carried out using a Hewlett-Packard 6890 gas chromatograph coupled to a 5971 quadrupole mass detector operating in electronic impact (EI) mode at 70 eV (both from Hewlett-Packard, Palo Alto, CA, USA). A 25 m × 0.25 mm i.d. ×

(29) Rajasekaran, A.; Thampi, P. P. *Eur. J. Med. Chem.* **2005**, *40*, 1359.
(30) Shaban, M. A. E.; Nasr, A. Z. *Adv. Heterocycl. Chem.* **1997**, *68*, 333.
(31) (a) Ellis, J. L.; Harman, D.; González, J.; Spera, M. L.; Liu, R.; Shen, T. Y.; Wypij, D. M.; Zuo, F. *J. Pharmacol. Exp. Ther.* **1999**, *288*, 1143. (b) Duttaroy, A.; Gomeza, J.; Gan, J.-W.; Siddiqui, N.; Basile, A. S.; Harman, W. D.; Smith, P. L.; Felder, C. C.; Levey, A. I.; Wess, J. *Mol. Pharmacol.* **2002**, *62*, 1084.
(32) Giese, B.; González-Gómez, J. A.; Witzel, T. *Angew. Chem., Int. Ed. Engl.* **1984**, *23*, 69.

0.25 mm film thickness fused silica column coated with SPB-1 (cross-linked methyl silicone) from Supelco (Bellefonte, PA, USA) was used. Mass spectra were recorded on a GC/MS spectrometer with an API-ES ionization source. Elemental analyses were performed at CQO (CSIC, Spain). TLC was performed on silica F254 and detection by UV light at 254 nm or by charring with ninhydrin, anisaldehyde, or phosphomolybdic-H_2SO_4 dyeing reagents. Where anhydrous solvents were needed, they were purified following the usual procedures. In particular, anh. DMF was critical for the outcome of the cyclization reaction and was either distilled at reduced pressure, bought from Aldrich or purified through a *Pure solv* PS-400-3-MD model. Column chromatography was performed on silica gel 60 (230 mesh).

Reaction of Compound 1 with *tert*-Butylisocyanide. To a solution of bromide **1** (270 mg, 0.99 mmol) in dry *t*-BuOH (27 mL, 0.037 M) at 40 °C, under argon, were successively added *tert*-butylisocyanide (2.29 mL, 20 equiv), AIBN (16.3 mg, 0.1 equiv), and Bu_3SnCl (0.03 mL, 0.1 equiv). $NaBH_3CN$ was then added in six equal portions, one every 30 min (total: 131 mg, 2 equiv). After the first addition, the reaction mixture was refluxed. After 24 h the mixture was allowed to reach room temperature and workup was performed. After addition of CH_2Cl_2 and a 3% aqueous solution of NH_3, the mixture was vigorously stirred. Then brine was added, and the aqueous phase was extracted with CH_2Cl_2 (×4). The organic phases were dried over Na_2SO_4, and the solvent was evaporated. The resulting residue was dissolved in ethyl ether, and then an I_2/ether solution was added, until the yellow color was permanent. The solution was thoroughly washed with a saturated aqueous solution of KF, the organic phase was dried, and the solvent was evaporated. The residue was taken up in acetonitrile and washed with small volumes of hexane (×3). The resulting crude was submitted to gradient column chromatography (CH_2Cl_2 → 3:10: 0.3 $CH_2Cl_2/CH_3OH/NH_3$), affording *exo*-nitrile **2** (77.7 mg, 36%), *endo*-nitrile **3** (3.6 mg, 2%), and amine **4** (19.6 mg, 7%).

***exo*-2-Cyano-7-(2,2,2-trifluoroacetyl)-7-azabicyclo[2.2.1]heptane (2).** oil; IR (KBr) ν 2962, 2242, 1694, 1463, 1244, 1192, 1138 cm^{-1}; ^1H NMR ($CDCl_3$, 300 MHz) δ 5.04 (d, J = 3.3 Hz, 1H, H1), 4.90 (t, J = 4.3 Hz, 1H, H4), 4.76 (s, 1H, H1′), 4.66 (s, 1H, H4′), 2.83 (dd, J = 4.9, 8.9 Hz, 1H, H2), 2.77 (dd, J = 4.8, 9.0 Hz, 1H, H2′), 2.30−1.82 (m, 8H, $H5_{exo}$, $H6_{exo}$, 2H3, both invertomers), 1.74−1.50 (m, 4H, $H5_{endo}$, $H6_{endo}$, both invertomers); ^{13}C NMR ($CDCl_3$, 100 MHz) δ 152.9 (q, $^2J_{C-F}$ = 38.3 Hz, N*C*OCF$_3$), 120.0, 119.7 (C'N, both invertomers), 116.1 (q, $^1J_{C-F}$ = 288.0 Hz, NCO*C*F$_3$), 60.0 (C1), 58.3 (C1′), 56.4 (C4), 54.4 (C4′), 37.1 (C3), 35.1 (C3′), 32.9 (C2), 31.1 (C2′), 29.6 (C5*, both invertomers), 27.5 (C6*), 27.4 (C6′*); MS (ES) m/z $[M + 1]^+$ 219.1, $[M + 23]^+$ 241.1. Anal. Calcd for $C_9H_9F_3N_2O$: C, 49.55; H, 4.16; N, 12.84. Found: C, 49.41; H, 4.40; N, 12.59.

***endo*-2-Cyano-7-(2,2,2-trifluoroacetyl)-7-azabicyclo[2.2.1]heptane (3).** oil; IR (KBr) ν 2966, 2244, 1699, 1461, 1230, 1188, 1158 cm^{-1}; ^1H NMR ($CDCl_3$, 400 MHz) δ 4.95 (t, J = 4.6 Hz, 1H, H1), 4.85 (t, J = 4.5 Hz, 1H, H4), 4.70 (s, 1H, H1′), 4.61 (s, 1H, H4′), 3.09−2.99 (m, 2H, H2), 2.43−2.17 (m, 4H, H3A, H5A), 2.10−1.69 (m, 8H, H3B, H5B, 2H6); ^{13}C NMR ($CDCl_3$, 125 MHz) δ 153.5 (q, $^2J_{C-F}$ = 38.4 Hz, N*C*OCF$_3$), 153.1 [q, $^2J_{C-F}$ = 38.4 Hz, (N*C*OCF$_3$)′], 119.4, 119.2 (C'N), 116.2 (q, $^1J_{C-F}$ = 288.3 Hz, NCO*C*F$_3$), 58.2 (br, C1), 57.5 (br s, with multiplicity, C4), 56.6 (C1′), 55.5 (C4′), 36.7 (C3*), 34.6 (C3′*), 31.6 (C2), 30.4 (C5*), 29.7 (C2′), 28.3 (C5′*), 26.8 (C6*), 24.6 (C6′*); MS (EI) m/z [M + 39]$^+$ 257. Anal. Calcd for $C_9H_9F_3N_2O$: C, 49.55; H, 4.16; N, 12.84. Found: C, 49.22; H, 4.40; N, 12.61.

2-*tert*-Butylaminomethyl-7-(2,2,2-trifluoroacetyl)-7-azabicyclo-[2.2.1]heptane (4). oil; IR (film) ν 3327, 2965, 1694, 1463, 1362, 1195, 1146 cm^{-1}; ^1H NMR ($CDCl_3$, 400 MHz) δ 4.68 (t, J = 4.6 Hz, 1H, H4), 4.58 (d, J = 4.0 Hz, 1H, H1), 4.44 (s, 1H, H4′), 4.39 (s, 1H, H1′), 2.38−2.24 (m, 2H, CH_2N), 1.93−1.77 (m, 3H, $H5_{exo}$, $H6_{exo}$, H2), 1.77−1.65 (m, 1H, $H3_{endo}$), 1.63−1.45 (m, 2H, $H5_{endo}$, $H6_{endo}$), 1.44−1.36 (m, 1H, $H3_{endo}$), 1.33−1.25 (m, 1H, H3′$_{endo}$), 1.04 (s, 9H, *t*-Bu); ^{13}C NMR ($CDCl_3$, 100 MHz) δ 153.2, 153.1 (2xq, $^2J_{C-F}$ = 37.1 Hz, N*C*OCF$_3$, smaller signals of each quadruplet hidden by noise), 116.7, 116.6 (2xq, $^1J_{C-F}$ = 288.2 Hz, NCO*C*F$_3$), 60.0 (C1), 57.8 (C1′), 57.4 (C4), 55.1 (C4′), 50.4, 50.3 [*C*(CH$_3$)$_3$], 46.6 (CH_2N), 45.0 (C2), 43.5 (C2′), 36.2 (C3), 34.5 (C3′), 30.1 (C5*), 29.1, 29.0 [2x (CH$_3$)$_3$], 28.1 (C6*), 27.9 (C6′*); MS (ES) m/z $[M + 1]^+$ 279.0, $[M + 23]^+$ 301.0. Anal. Calcd for $C_{13}H_{21}F_3N_2O$: C, 56.10; H, 7.61; N, 10.07. Found: C, 55.98; H, 7.45; N, 9.96.

***N*-(*tert*-Butyl)-2,2,2-trifluoro-*N*-{[7-(2,2,2-trifluoroacetyl)-7-azabicyclo[2.2.1]hept-2-yl]methyl}acetamide (5).** Amine **4** (30 mg, 0.11 mmol) was treated with trifluoroacetic acid anhydride (2 mL, 14.4 mmol) and pyridine (2 mL) for 24 h at room temperature. Then the solvents were evaporated under reduced pressure and coevaporated with toluene. The resulting crude was purified through column chromatography (100:3:0.5 CH_2Cl_2/MeOH/NH_3) to yield compound **5** (34 mg, 83%) as a yellow solid: mp 111−113 °C; IR (KBr) ν 2968, 1687, 1470, 1191, 1147 cm^{-1}; ^1H NMR ($CDCl_3$, 400 MHz) δ 4.81−4.75 (m, 1H, H1), 4.54 (s, 1H, H4), 4.51 (d, J = 4.4 Hz, 1H, H1′), 4.23−4.18 (br s, 1H, H4′), 3.64 (dd, J = 5.1, 15.8 Hz, 1H, CH_2N, minor invertomer), 3.54 (dd, J = 6.6, 15.9 Hz, 1H, CH_2N, major invertomer), 3.23 (dd, J = 10.4, 15.7 Hz, 1H, CH_2N, minor invertomer), 3.17 (dd, J = 8.5, 15.9 Hz, 1H, CH_2N, major invertomer), 2.32−2.16 (m, H2), 1.97−1.81 (m, 2H5*), 1.77−1.66 (m, H3B), 1.66−1.52 (m, 2H6, H3B), 1.48, 1.46 (2s, 9H, *t*Bu); ^{13}C NMR ($CDCl_3$, 100 MHz) δ 158.0, 153.8 (q, $^2J_{C-F}$ = 37.3 Hz, N*C*OCF$_3$), 116.5 (q, $^1J_{C-F}$ = 288.1 Hz, NCO*C*F$_3$), 60.6 (C1), 59.6, 59.5 [*C*(CH$_3$)], 57.9, 57.4 (C4), 55.3 (C1′), 47.6 (q, $^4J_{C-F}$ = 3.0 Hz, CH_2N), 47.5 [br s, (CH$_2$N)′], 45.1, 43.7 (C2), 34.9, 32.6 (C3), 30.3, 30.2 (C5*), 28.3 [(CH$_3$)$_3$], 28.2, 28.1 (C6*); MS (ES) m/z $[M - 55]^+$ 319.0, $[M + 1]^+$ 375.2, $[M + 23]^+$ 397.0. Anal. Calcd for $C_{15}H_{20}F_6N_2O_2$: C, 48.13; H, 5.39; N, 7.48. Found: C, 48.30; H, 5.15; N, 7.41.

2-(2*H*-Tetrazol-5-yl)-7-(trifluoroacetyl)-7-azabicyclo[2.2.1]heptane (7). To a solution of nitrile **2** (34.3 mg, 0.16 mmol) in dry toluene (0.6 mL, 0.26 M), under argon, were added $TMSN_3$ (0.05 mL, 0.36 mmol, 2.3 equiv) and Bu_2SnO (25 mg, 0.098 mmol, 0.63 equiv). The tube was sealed, and the mixture was heated for 19 h at 120 °C and cooled to room temperature. The solvent was removed, AcOEt was added and washed with an aqueous $NaHCO_3$ 10% solution (×2). The aqueous layer was acidified to pH 2 with an aqueous HCl 5% solution and extracted with AcOEt (×3). The organic phase was dried with $MgSO_4$. The crude was submitted to column chromatography (10% → 20% CH_2Cl_2/MeOH) to give tetrazole **7** (35.6 mg, 87%): oil; IR (film) ν 3416, 2963, 1693, 1471, 1247, 1194, 1155 cm^{-1}; ^1H NMR ($CDCl_3$, 300 MHz) δ 8.47 (br s, 1H, NH), 5.06−4.98 (m, H1, major invertomer), 4.97−4.89 (m, H4, minor invertomer), 4.74 (br s, H4, major invertomer), 4.59 (br s ancho, H1, minor invertomer), 3.76 (dd, J = 4.4, 8.8 Hz, 1H, H2, minor invertomer), 3.63 (dd, J = 5.1, 8.2 Hz, 1H, H2, major invertomer), 2.50−2.14 (m, 2H, 2 × H3), 2.14−1.66 (m, 4H, 2 × H5, 2 × H6); ^{13}C NMR ($CDCl_3$, 125 MHz) δ 159.9, 159.6 (C5′), 153.4 (q, $^2J_{C-F}$ = 37.4 Hz, N*C*OCF$_3$, major invertomer), 153.3 (q, $^2J_{C-F}$ = 37.9 Hz, N*C*OCF$_3$, minor invertomer), 116.4 (q, $^1J_{C-F}$ = 287.4 Hz, NCO*C*F$_3$, major invertomer), 116.2 (q, $^1J_{C-F}$ = 287.8 Hz, NCO*C*F$_3$, minor invertomer), 62.6 (C1, minor invertomer), 59.8 (C1, major invertomer), 57.8 (C4, minor invertomer), 55.6 (C4, major invertomer), 39.1 (C2, minor invertomer), 37.8 (C3, minor invertomer), 37.3 (C2, major invertomer), 35.0 (C3, major invertomer), 29.8 (C5*, minor invertomer), 29.6 (C5*, major invertomer), 27.9 (C6*, minor invertomer), 27.8 (C6*, major invertomer); MS (ES) m/z $[M + 1]^+$ 262.0, $[M + 23]^+$ 284.0, $[2M + 23]^+$ 545.0. Anal. Calcd for $C_9H_{10}F_3N_5O$: C, 41.38; H, 3.86; N, 26.81. Found: C, 41.11; H, 3.75; N, 26.70.

2-(2*H*-Tetrazol-5-yl)-7-azabicyclo[2.2.1]heptane (8). To a solution of tetrazole **7** (13.7 mg, 0.05 mmol) in a mixture of methanol (1 mL) and water (0.5 mL) was added K_2CO_3 (36.6 mg, 0.26 mmol, 5 equiv), and the mixture was stirred at room temperature for 24 h. The solvents were removed, and the residue was purified by column chromatography (30% CH_2Cl_2/MeOH) affording tetrazole **8** (7.1

mg, 82%) as a white solid: mp 290 °C (dec); IR (KBr) ν 3430, 3134, 2961, 2498, 1635, 1472, 1388 cm^{-1}; ^1H NMR (CD_3OD, 300 MHz) δ 4.92 (s, 2H, 2 × NH), 4.42 (d, J = 3.8 Hz, 1H, H1), 4.27 (t, J = 4.2 Hz, 1H, H4), 3.52 (dd, J = 5.0, 9.3 Hz, 1H, H2), 2.36 (dd, J = 9.3, 13.3 Hz, 1H, $H3_{endo}$), 2.22 (dm, J = 13.3 Hz, 1H, $H3_{exo}$), 2.18−1.79 (m, 4H, 2 × H5, 2 × H6); ^{13}C NMR (CD_3OD, 75 MHz) δ 164.6 (C5′), 64.5 (C1), 60.0 (C4), 38.6 (C2), 36.8 (C3), 27.8, 27.6 (C5, C6); EM (ES) m/z $[M + 1]^+$ 166.1, $[M + 23]^+$ 188.1. HRMS calcd for $C_7H_{12}N_5$ 166.1087 ($M + H^+$), found 166.1077 ($M + H^+$).

2-(5-Methyl-1,3,4-oxadiazol-2-yl)-7-(trifluoroacetyl)-7-azabicyclo[2.2.1]heptane (9). A solution of tetrazole **7** (30 mg, 0.11 mmol) in acetic anhydride (0.4 mL, 4.23 mmol, 37.0 equiv) was heated at 135 °C for 1 h. Then water was added, and the solvents were removed. The residue was purifed by column chromatography, to give oxadiazole **9** (20.7 mg, 66%): oil; IR (film) ν 2964, 1697, 1595, 1568, 1461, 1249, 1192, 1145 cm^{-1}; ^1H NMR ($CDCl_3$, 500 MHz) δ 4.93 (s, 1H, 2 invertomers, H1*, H4*), 4.68 (s, 1H, 2 invertomers, H1♦*, H4♦*), 3.31 (dd, J = 4.8, 8.9 Hz, 1H, H2), 3.24 (dd, J = 4.6, 9.0 Hz, 1H, H2♦), 2.50, 2.49 (2s, 3H, 2 invertomers, CH_3), 2.55−2.37 (m, 1H, $H3_{exo}$), 2.17−1.89 (m, 3H, $H3_{endo}$, $H5_{exo}$, $H6_{exo}$), 1.87−1.63 (m, 2H, $H5_{endo}$, $H6_{endo}$); ^{13}C NMR ($CDCl_3$, 125 MHz) δ 166.9, 166.8 (C2′), 164.6, 164.5 (C5′), 153.1 (q, $^2J_{C-F}$ = 37.6 Hz, N*C*OCF$_3$), 152.9 (q, $^2J_{C-F}$ = 37.5 Hz, NCOCF$_3$), 116.4 (q, $^1J_{C-F}$ = 288.0 Hz, NCO*C*F$_3$), 116.2 (q, $^1J_{C-F}$ = 288.2 Hz, NCO*C*F$_3$), 60.8 (q, $^3J_{C-F}$ = 2.6 Hz, C1♦*), 58.8 (C1*), 57.0 (q, $^3J_{C-F}$ = 2.8 Hz, C4♦*), 55.0 (C4*), 40.3, 38.6 (C2), 35.7, 33.9 (C3), 30.2, 30.1 (C5*), 27.9 (C6*), 11.2, 11.0 (CH_3); MS (ES) m/z $[M + 1]^+$ 276.2, $[M + 23]^+$ 298.3, $[2M + 23]^+$ 573.5. Anal. Calcd for $C_{11}H_{12}F_3N_3O_2$: C, 48.00; H, 4.39; N, 15.27. Found: C, 48.04; H, 4.81; N, 15.38.

2-(5-Methyl-1,3,4-oxadiazol-2-yl)-7-azabicyclo[2.2.1]heptane (10). To a solution of trifluoroacetamide **9** (6 mg, 0.02 mmol) in a mixture of water (0.1 mL) and methanol (0.25 mL, 0.062 M) was added K_2CO_3 (15.5 mg, 0.112 mmol, 5.1 equiv), and the reaction mixture was stirred at room temperature for15 h. The solvents were evaporated, and the residue was purified by column chromatography (5% CH_2Cl_2/MeOH) to give compound **10** (3 mg, 77%): oil; ^1H NMR ($CDCl_3$, 500 MHz) δ 3.91−3.85 (m, 2H, H1, H4), 3.13 (dd, J = 4.9, 8.8 Hz, 1H, H2), 2.51 (s, 3H, CH_3), 2.50 (br s, 1H, NH), 2.08 (dm, J = 12.5 Hz, 1H, $H3_{exo}$), 1.96 (dd, J = 8.8, 12.5 Hz, 1H, $H3_{endo}$), 1.86−1.71 (m, 2H, $H5_{exo}$, $H6_{exo}$), 1.55−1.39 (m, 2H, $H5_{endo}$, $H6_{endo}$); ^{13}C NMR ($CDCl_3$, 125 MHz) δ 169.4, 164.1 (C2′, C5′), 61.1, 56.5 (C1, C4), 39.9 (C2), 36.9 (C3), 29.3, 28.9 (C5, C6), 11.2 (CH_3). HRMS calcd for $C_9H_{14}N_3O$ 180.1131 ($M + H^+$), found 180.1125 ($M + H^+$).

3-{7-(2,2,2-Trifluoroacetyl)-7-azabicyclo[2.2.1]heptan-2-yl}propanenitrile (13). To a solution of bromide **1** (112 mg, 0.41 mmol) in dry toluene (1 mL, 0.4 M), under argon and at room temperature, AIBN (5 mg) and acrylonitrile (0.14 mL, 2.12 mmol, 5 equiv) were added; then, argon was bubbled for 15 min to deoxygenate the mixture. A mixture of $HSnBu_3$ (0.13 mL, 0.47 mmol, 1.1 equiv), and AIBN (10 mg) in dry, deoxygenated toluene (0.7 mL) was added slowly for 2 h at 90 °C (bath temperature). After the addition, the reaction was heated at 90 °C for 22 h. Then, the mixture was cooled at room temperature, the solvent was evaporated, and the residue was dissolved in ethyl ether, treated with a solution of iodine in ether until permanent color, and washed with a saturated aqueous KF solution. The organic phase was dried with $MgSO_4$, filtered, and the solvent was removed. The crude mixture was submitted to flash chromatography (0.25% CH_2Cl_2/MeOH) to give cyanide **13** (84% as measured by GC/MS): oil; IR (film) ν 2956, 2247, 1691, 1468, 1195, 1146 cm^{-1}; ^1H NMR ($CDCl_3$, 400 MHz) δ 4.77 (t, J = 4.7 Hz, H1*, major invertomer), 4.56−4.51 (m, H1*, minor invertomer, H4*, major invertomer), 4.27−4.22 (m, H4*, minor invertomer), 2.48−2.30 (m, 2H, 2 × H2′), 2.12−2.00 (m, 1H, H2), 1.98−1.33 (m, 8H); ^{13}C NMR ($CDCl_3$, 100 MHz) δ 153.5 (q, $^2J_{C-F}$ = 37.3 N*C*OCF$_3$), 119.1 (CN, major invertomer), 119.0 (CN, minor invertomer), 116.6 (q, $^1J_{C-F}$ = 288.2 Hz, NCO*C*F$_3$, major invertomer), 116.5 (q, $^1J_{C-F}$ = 288.3 Hz, NCO*C*F$_3$, minor invertomer), 60.9 (q, $^4J_{C-F}$ = 2.4 Hz, C1*, minor invertomer), 58.5 (C1*, minor invertomer), 57.6 (q, $^4J_{C-F}$ = 2.6 Hz, C4*, major invertomer), 55.3 (C4*, major invertomer), 42.3, 40.9 (C2), 37.8, 35.8, 30.4, 30.2, 30.1, 30.0, 28.0, 27.9, 15.4 (C2′, major invertomer), 15.2 (C2′, minor invertomer); MS (ES) m/z $[M + 1]^+$ 247.0, $[M + 23]^+$ 269.0. Anal. Calcd for $C_{11}H_{13}F_3N_2O$: C, 53.66; H, 5.32; N, 11.38. Found: C, 53.45; H, 5.21; N, 11.36.

2-[2-(2*H*-Tetrazol-5-yl)ethyl]-7-(trifluoroacetyl)-7-azabicyclo[2.2.1]heptane (14). To a solution of cyanide **13** (36.1 mg, 0.147 mmol) in dry toluene (0.5 mL, 0.29 M), under argon, $TMSN_3$ (0.04 mL, 0.293 mmol, 2.0 equiv) and Bu_2SnO (19.2 mg, 0.076 mmol, 0.51 equiv) were added. The mixture was heated at 120 °C for 23 h in a sealed tube. Then, the solvent was evaporated, the residue was dissolved in AcOEt, washed with 10% aqueous $NaHCO_3$ solution (×2), the aqueous extract was treated with 5% aqueous HCl solution until pH 2, and the mixture was extracted with AcOEt (×3). The organic phase was dried over $MgSO_4$, filtered and evaporated. The residue was submitted to chromatography (6% CH_2Cl_2: MeOH) to give compound **14** (36.5 mg, 86%): oil; ^1H NMR ($CDCl_3$, 400 MHz) δ 4.74 (d, J = 4.6 Hz, H1*, minor invertomer), 4.58−4.51 (m, H1*, H4*, major invertomer), 4.30−4.26 (m, H4*, minor invertomer), 3.13−3.02 (m, 2H, 2 × H2′), 2.03−1.39 (m, 10H); ^{13}C NMR ($CDCl_3$, 100 MHz) δ 156.1 (br, C5"), 153.5 (q, $^2J_{C-F}$ = 37.5 Hz, N*C*OCF$_3$, major invertomer), 153.1 (q, $^2J_{C-F}$ = 37.1 Hz, N*C*OCF$_3$, minor invertomer), 116.6 (q, $^1J_{C-F}$ = 287.5 Hz, NCO*C*F$_3$, major invertomer), 116.5 (q, $^1J_{C-F}$ = 287.9 Hz, NCO*C*F$_3$, minor invertomer), 61.6 (C1*, minor invertomer), 59.1 (C1*, major invertomer), 58.1 (C4*, minor invertomer), 55.8 (C4*, major invertomer), 42.6 (C2, minor invertomer), 41.4 (C2, major invertomer), 37.9 (C3♦, major invertomer), 35.8 (C3♦, minor invertomer), 33.0 (C5♦, major invertomer), 32.7 (C5♦, minor invertomer), 30.0 (C6♦, minor invertomer), 29.8 (C6♦, major invertomer), 27.9 (C1′♦, minor invertomer), 27.8 (C1′♦, major invertomer), 21.5 (C2′, major invertomer), 21.1 (C2′, minor invertomer). HRMS calcd for $C_{11}H_{15}F_3N_5O$ 290.1223 ($M + H^+$), found 290.1225 ($M + H^+$).

2-[2-(2*H*-Tetrazol-5-yl)ethyl]-7-azabicyclo[2.2.1]heptane (15). To a solution of tetrazole **14** (15.3 mg, 0.053 mmol) in methanol: water (5:2, 0.85 mL, 0.062 M), K_2CO_3 (38.1 mg, 0.276 mmol, 5.2 equiv) was added, and the mixture was stirred for 16 h at room temperature; then, the solvents were removed, and the residue was submitted to chromatography (CH_2Cl_2: MeOH, 25%) to afford compound **15** (9.4 mg, 92%) as a white solid: mp 240 °C (dec.); ^1H NMR (CD_3OD, 400 MHz) δ 4.09 (t, J = 4.3 Hz, 1H, H4), 3.86 (d, J = 3.9 Hz, 1H, H1), 2.77 (t, J = 7.5 Hz, 2H, 2 × H2′), 1.97−1.75 (m, 5H, H1′, H2, $H3_{endo}$, $H5_{exo}$, $H6_{exo}$), 1.67−1.54 (m, 3H, H1′, $H5_{endo}$, $H6_{endo}$), 1.50−1.45 (m, 1H, $H3_{exo}$); ^{13}C NMR (CD_3OD, 100 MHz) δ 162.4, 62.7 (C1), 60.2 (C4), 40.2 (C2), 36.4 (C3), 34.6 (C1′), 28.3, 27.1 (C5, C6), 23.8 (C2′); HRMS calcd for $C_9H_{16}N_5$ 194.1400 ($M + H^+$), found 194.1401 ($M + H^+$).

Computational Methods. The calculations have been performed with Gaussian03 suite of programs.[35] The geometries have been fully optimized at DFT level by means of the B3LYP hybrid functional.[36] The standard 6-31G(d) basis set has been applied for all the atoms except Sn. Sn atom has been described by LANL2DZ basis set,[37] where the innermost electrons are replaced by a relativistic ECP. To get reliable energy values, single-point-energy calculations have been carried out with the extended 6-311G(2d,p) basis set on the optimized structures. Zero-point energies (ZPEs) and thermal contributions to thermodynamic functions and activa-

(33) We have also investigated the free radical allylation[34] of bromide **1**, a reaction that provided the expected 1-(2-allyl-7-azabicyclo[2.2.1]heptan-7-yl)-2,2,2-trifluoroethanone (**16**) in an incomplete and low yielding reaction (see Supporting Information Available).

(34) Keck, G. E.; Yates, J. B. *J. Org. Chem.* **1982**, *47*, 359.

(35) *Gaussian 03, Revision B.03*; Frisch, M. J. et al. Gaussian, Inc.: Wallingford, CT, 2003.

tion parameters were computed at the same level on the optimized structures, and harmonic frequencies by using the rigid rotor/harmonic oscillator approximation and the standard expressions for an ideal gas in the canonical ensemble at 298.15 K and 1 atm. The transition states were verified to have only one imaginary frequency and hence correspond to a first-order saddle point on the potential energy surface.

In some cases, the whole step path was traced by using the intrinsic reaction coordinate (IRC) at the optimization level. The IRC calculation started from the optimized transition structure and followed the reaction path in both directions, toward the two minima it connects.

Solvent effects have been taken into account by the self-consistent reaction field (SCRF) method using the so-called conductor polarizable continuum model (CPCM)[38] as implemented in Gaussian03, in which the solvent is represented by an infinite dielectric medium characterized by the relative dielectric constant of the bulk. A relative permittivity of 10.9 was assumed to simulate *tert*-butanol as solvent.

The natural bond orbital (NBO) analyses[39] have been performed by the module NBO v.3.1 implemented in Gaussian03 to evaluate the NPA charges and hyperconjugation effects.

Acknowledgment. E.G.S. is an I3P-CSIC fellow. J.M.C. thanks MEC (Spain) for a grant (SAF2006-08764-C02-01), Comunidad de Madrid (S/SAL-0275-2006), Instituto de Salud Carlos III [RED RENEVAS (RD06/0026/1002)].

Supporting Information Available: NMR spectra for all new compounds, experimental methods and spectroscopic data for the synthesis of triazoloepibatines (**IV**), procedures for the reaction of compound **1** with *tert*-butylisocyanid*e* (Table 2), and the reaction of bromide **1** with allyltributylstannane, computational details (Tables 3−7, Charts 1−3), Cartesian coordinates, and ref 35. This material is available free of charge via the Internet at http://pubs.acs.org.

JO8011094

(36) (a) Lee, C.; Yang, W.; Parr, R. *Phys. Rev. B* **1988**, *37*, 785–789. (b) Becke, A. *J. Chem. Phys.* **1993**, *98*, 5648.
(37) Hay, P. J.; Wadt, W. R. *J. Chem. Phys.* **1985**, *82*, 270.
(38) (a) Barone, V.; Cossi, M. *J. Phys. Chem. A* **1998**, *102*, 1995–2001. (b) Cossi, M.; Rega, N.; Scalmani, G.; Barone, V. *J. Comput. Chem.* **2003**, *24*, 669.
(39) (a) Reed, A. E.; Weinhold, F. *J. Chem. Phys.* **1983**, *78*, 4066–4073. (b) Reed, A. E.; Curtiss, L. A.; Weinhold, F. *Chem. Rev.* **1988**, *88*, 899.